Effects of Polymorph Transformation via Mercerisation on Microcrystalline Cellulose Fibres and Isolation of Nanocrystalline Cellulose Fibres

SaifulAzry, S. O. A.[1]*, Chuah, T. G.[1,2], Paridah M. T.[1,3], Aung, M. M.[1,4] and Edi S. Z.[1,2]

[1]*Higher Institution Centre of Excellence Wood and Tropical Fibre,*
Institute of Tropical Forestry and Forest Products, Universiti Putra Malaysia, 43400 UPM, Serdang, Selangor, Malaysia
[2]*Faculty of Engineering, Universiti Putra Malaysia, 43400 UPM, Serdang, Selangor, Malaysia*
[3]*Faculty of Forestry, Universiti Putra Malaysia, 43400 UPM, Serdang, Selangor, Malaysia*
[4]*Faculty of Science, Universiti Putra Malaysia, 43400 UPM, Serdang, Selangor, Malaysia*

ABSTRACT

Cellulose I can be irreversible transformed into cellulose II via mercerisation or regeneration treatments. In the past few decades, mercerisation was used mainly to improve fibre properties for textile industries. A few studies have focused on the effects of mercerisation treatment on the cellulose polymorph itself and after it was downscaled to nanosize. This study aims to characterise the micro size crystalline cellulose after complete polymorph conversion via mercerisation technique and investigate its effects on isolation to nanosize crystalline cellulose. A microcrystalline cellulose (MCC) was purchased and converted into cellulose II via mercerisation technique. Sulphuric acid hydrolysis was carried-out to produce nanocrystalline cellulose (NCC). The MCC and NCC of different polymorphs were then characterised and analysed for its crystallography, morphology, particles size distribution and thermal stability using wide-angle X-ray diffraction (WXRD), electron microscopes, dynamic light scattering analyser and thermogravimetric analyser, respectively. Both MCC and NCC fibres showed complete conversion of cellulose I to cellulose II and decrement of crystallinity index (CI). Electron micrographs revealed that both cellulose II polymorph fibres (MCC II and NCC II) were morphological affected. The analysis of size distribution and dimension measurement confirmed that mercerisation treatment causing increment in fibre diameter and shortened length. The thermal stability of both cellulose II polymorph fibres (MCC II and NCC II) was also found to be improved.

Keywords: Nanocrystalline cellulose, microcrystalline cellulose, mercerization, alkaline treatment, cellulose polymorph

INTRODUCTION

Cellulose consists of β-1, 4-D- linked glucose chains present in 4 crystalline polymorphs (cellulose I, II, III and IV) based on their unit cell dimension (Yue, 2011; Mansikkamäki et al., 2005, pp. 383-389). Among all cellulose polymorphs, cellulose I and II are most widely discussed and studied. Cellulose I can be irreversible transformed into cellulose II by the mercerization or regeneration treatments. Cellulose I is also called native cellulose because it is the most cellulose polymorph found in nature and coexists in two sub-allomorphs; cellulose Iα and Iβ (Prasanth et al., 2015, pp. 311-340; Kenji, 2005). Cellulose from bacterial and algae comprised dominantly by cellulose Iα whereas cellulose from higher plants and tunicate mostly composed by cellulose Iβ (Wertz et al., 2010). Cellulose I and II polymorphs can be reversible transformed into cellulose III polymorph using liquid ammonia or anhydrous ethylamine treatment and cellulose IV polymorph by high temperature treatment - annealed.

As mentioned above, cellulose I polymorph can be irreversible transformed into cellulose II via two different routes: regeneration treatment and mercerisation. Regeneration treatment involves dissolving the cellulose in derivative-forming solvent and then reprecipitating by dilution in water. Meanwhile, mercerisation (which is also called alkalisation treatment) is a process that involvos soaking of cellulose in aqueous solution of alkalies such as NaOH, LiOH, KOH, RbOH and CsOH. Mercerisation becomes preferable and widely used due to its simple procedure and cost effective. Among alkalies that are used for mercerisation, sodium hydroxide (NaOH) is the most widely used. Other than transformation treatment, cellulose II also can be produced using bacteria *Gluconacetobacter xylinus* (Jin et al., 2016, pp. 327-335; Kuga et al., 1993, pp. 3293-3297).

The polymorph transformation treatment caused rearrangement of cellulose I crystal lattice from parallel order into antiparallel order in cellulose II (Revol et al., 1987, pp. 1274-1275). The hydrogen bonding in cellulose II is more complex than cellulose I. In cellulose II, hydrogen bonds connect all of the neighbouring cellulose molecules, whereas in cellulose I, van der Waals forces are responsible for its sheet structure (Borysiak & Grząbka-Zasadzińska, 2016). The anti-parallel chain in cellulose II enables the formation of not only inter-chain but also of inter-plane hydrogen bonds (Gupta et al., 2013, pp. 843-849). The polymorphic transformation is usually observed by X-ray diffraction peak which peaks on about $2\theta = 14.7°$, $16.4°$, $22.5°$, and $34.4°$ indicating cellulose I structure and $2\theta = 12.1°$, $20.0°$ and $21.7°$ from cellulose II structure, respectively (Mansikkamäki et al., 2005, pp. 233-242).

The polymorphic and morphological transformations of cellulose are strongly associated with their properties and applications (Jin et al., 2016, pp. 327-335). Due to the different super molecular structures, cellulose I and II possess different properties and advantages over the other. Chemically, cellulose II has higher thermal stability and chemical reactivity, which offer benefits in terms of functionality. Meanwhile, cellulose I exhibits much better mechanical properties (Liu & Hu, 2008, pp. 735-739; Široký et al., 2010, pp. 103-115; Wang, et al., 2014, pp. 1505-1515). As cellulose II has some preferable properties over cellulose I, it has been widely used in some industries such as textile, pulp and paper, pharmaceutical and biocomposites (Kumar et al., 2002, pp. 129-140; Ma et al., 2011, pp. 383-389; Yue et al., 2015, pp. 438-447).

During mercerisation treatment, three phases are undertaken: micro-fibril swelling, crystalline area disruption, and new crystalline lattice formation (Yue et al., 2012, pp. 1173-1187). Once mercerisation treatment is started, the alkalies penetrate and convert the entire fibre into a swollen state. Consequently, the assembly and orientation of microfibrils are completely disrupted. The new crystalline lattice was formed from the original parallel-chain crystal structure of cellulose I dominated by O6-H-O3 inter-chain bonding was transformed into anti-parallel chains of cellulose II, which is dominated by O6-H-O2 inter-chain bonding. The intra-chain hydrogen bond in both polymorphs remains the same with O3-H-O5 bond which gives cellulose chain its rigidity and linear shape (Dinand et al., 2002, pp. 7-18). Since cellulose II involves chain folding (Langan et al., 1999, pp. 9940-9946), the structure is more difficult to unravel and the reverse transformation from cellulose II to cellulose I does not occur (Revol et al., 1987, pp. 1724-1725). Mercerisation depends on the conditions during the treatment: alkali concentration, temperature, time, additive and the tension of materials (Yue, 2011). The concentrations of NaOH between 10 to 15 wt.% (Borysiak & Grząbka-Zasadzińska, 2016) and up to 20 wt.% (Yue et al., 2015, pp. 438-447) are optimum for complete transformation of cellulose I into cellulose II. Other than polymorphic transformation, mercerisation treatment is also capable of removing hemicellulose and impurities. Thus, it promotes better interfacial bonding between fibres and resin in composite applications (Borysiak & Doczekalska, 2008, pp. 101-103).

The hierarchical structure design of cellulose fibre exhibits uniqueness to its properties. The mechanical performance of cellulose fibre increases tremendously when it is downscaled from macro to nano level (Silva et al., 2015, pp. 427-460), thus, attracts great interest to use it in various fields such as material science, electronics, catalysis and biomedicine (Gatenholm & Klemm, 2010, pp. 208-213). Nanocellulose is divided into two types; nanofibrillated cellulose (NFC) and nanocrystalline cellulose (NCC). Each of them was produced using different extraction procedures and morphologies (Jonoobi et al., 2015, pp. 935-969). NCC shows a high specific strength, modulus and aspect ratio which attribute to the improvement of mechanical performance of composites, even at low loading percentage (Habibi et al., 2010, pp. 3479-3500). NCC was produced by acid hydrolysis and usually using hydrochloric acid or sulphuric acid. Sulphuric acid is preferable as it produces highly stable aqueous suspension that has negatively charged nanocrystals (Puglia et al., 2014, pp. 163-198). During hydrolysis, acid will attack the amorphous region of cellulose fibril, producing shorter chain fragments (individual nanocrystal) that comprise main crystalline region which possesses more resistance to acid attack (Habibi et al., 2010, pp. 3479-3500). The properties of NCC is dependent upon the cellulose, source, hydrolysis condition and pre-treatment (Lu & Hsieh, 2010, pp. 329-336; Liu et al., 2012, pp. 1449-1480).

In the past few decades, mercerisation was used mainly to improve fibre properties for the textile industries and it is used in many other applications as a pre-treatment only recently. However, most studies have focused on the treatment effects to the products being produced (i.e., composites). Meanwhile, a few studies have focused on the effects of the mercerisation treatment on the cellulose polymorph itself and after it was downscaled to nanosize. This study

aims to characterise the micro size crystalline cellulose after a complete polymorph conversion via mercerisation technique and investigate its effects on isolation to nanosize crystalline cellulose. Microcrystalline cellulose (MCC) was chosen due to its purity mainly on cellulose without any further process.

MATERIALS AND METHODS

Experimental Design

A process flow of the study is illustrated in Figure 1 below.
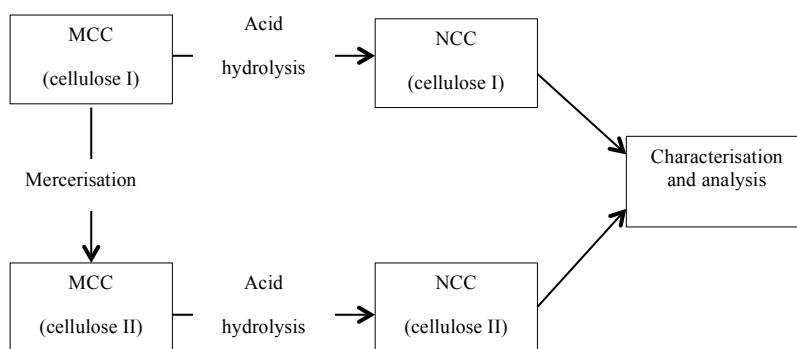
Figure 1. The process flow of cellulose polymorph conversion and isolation of nanocrystalline cellulose fibres.

Materials

A commercial microcrystalline cellulose (MCC) from wood pulp was purchased from Systerm Chemicals, Malaysia. Sodium hydroxide (NaOH) pellets and sulphuric acid (H2SO4) (concert. 95-98%) were supplied by R&M Chemicals, Malaysia.

Mercerisation

The conversion of cellulose polymorph was carried out by using the mercerisation technique. Raw MCC (MCC I) is a native cellulose that comprises mainly cellulose I. MCC I fibres were sieved (60 mesh) and about 60g of the sieved fibres were than used for mercerisation. The fibres then subjected to NaOH solution with the concentration of 20 wt.% for 4 hours at room temperature in a separating funnel. The slurry was then collected and filtered prior to washing until it reached a neutral pH value. The treated sample (MCC II) was then vacuum oven-dried at 40°C until it reached a constant weight (~ 48 hours).

Acid Hydrolysis

Acid hydrolysis procedure was adopted and modified from Bondeson et al. (2006, pp. 171-180). The fibres (MCC I and MCC II) were with the preheated H2SO4 solution 65% (w/w)

at 45°C for 60 min and vigorously stirred using a mechanical stirrer. The ratio of fibres (g) to acid (ml) was 1:10. The colloidal fibres were then diluted with tenfold of cold deionized water (4°C) to stop the hydrolysis. The acid was removed via separation by using Hermle Z306 centrifuge at 6000 rpm for 10 min for the first cycle and the aqueous layer was removed and replaced with new deionised water. The process was repeated for 30 min for each cycle until a cloudy suspension was obtained (~ 4-5 cycles). The suspension was then dialysed using a dialysis membrane until a neutral pH was reached. Subsequently, the dialysed suspension was homoginised using a IKA Ultra Turax T25 homogiser for 15 min, followed by freeze drying by Chemopharm-Labogene bench top freeze dryer. Both freeze dried nanofibres were then labelled as NCC I and NCC II, respectively.

Wide-Angle X-Ray Diffraction (WXRD)

X-ray diffraction analyses for micro and nanocrystalline cellulose polymorphs were carried out using an IS/APD2000 X-ray diffractometer. The diffraction pattern was collected in step scan mode in an angle range of 5 to 30°. The wavelength of the Cu/Ka radiation source was 1.5405 Å. The spectra was obtained at 30 mA with an accelerating voltage of 60 kV. X-ray diffraction data were analysed using the X'Pert HighScore software. The crystalline index (CI, %) of the samples was calculated using Segal et al.'s (1959, pp. 786-794) equation, as follows:

$$CI \% = [I_c / (I_c + I_a)] \times 100 \tag{1}$$

Where, I_c and I_a represent the intensity of lattice peak diffraction and amorphous regions, respectively. A diffraction around $2\theta = 22.5°$ was peak for plane (002) and the lowest intensity at a diffraction angle of around $2\theta = 18.0°$ was measured as the amorphous part.

Electron Microscopy

Scanning Electron Microscopy (SEM). The morphology of the MCC I and MCC II fibres were analyzed using scanning electron microscope, Hitachi S-34000N. The images were captured up to 1000 magnification and with 5kV accelerating voltage.

Field Emission Scanning Electron Microscopy (FE-SEM). The morphology of NCC I and NCC II was analysed using Jeol JSM 7600F Field Emission Scanning Electron Microscopy (FE-SEM). Glimmer plates were fixed with conducting carbon on a specimen holder. A drop of diluted fibre/water suspension (1:20) was put onto it. The samples were air dried and the remaining fibres were sputtered with a platinum layer. The images were taken up to 150k magnification with 5 kV accelerating voltage.

Transmission electron microscope (TEM). The size and shape images of NCC I and NCC II were studied under a transmission electron microscope (TEM) Hitachi model H-7100. A drop of diluted fibres suspension that was prior stained with 0.5% solution of uranyl acetate was deposited onto a carbon-coated grids plate, and allowed to dry at room temperature.

Fibre Size Distribution, Zeta-Potential and Conductivity Analyser Metasizer. The MCC-I and MCC-II fibre size were measured using Malvern 3000 Metasizer instrument at dry state.

Nano-Zetasizer. The nanocellulose fibre size, potential charges and conductivity were measured using Malvern Zetasizer instrument. Nanocellulose fibres suspension (0.05%) was prepared using deionised water and homogenised for 10 minutes prior to size and zeta potential-conductivity measurement at 25°C.

Thermogravimetric Analysis (TGA). Thermal stability of all MCC and NCC fibres was analysed using Thermogravimetric Analyzer (TGA Q500 - TA instruments) in a nitrogen atmosphere. About 5-10 mg of each samples were heated in a platinum pan at the temperatures of 35˚C to 600˚C and heating rate of 10˚C/min.

RESULTS AND DISCUSSION

Crystallography Analysis

The crystallography analysis using WXRD was carried out to confirm complete transformation of cellulose I polymorph into cellulose II polymorph after the mercerisation treatment. Besides polymorphic analysis, it also to determine the crystallinity of fibres after mercerisation and hydrolysis. The diffraction patterns of MCC before (MCC I) and after mercerisation (MCC II) and isolated nanocrystalline fibres (NCC I and NCC II) are shown in Figure 2. As observed, MCC I shows three peaks at $2\theta = 15.14°$, $16.55°$ and $22.63°$, respectively, which confirmed that only cellulose I was present. After the mercerisation treatment (MCC II), two weaker peaks were found to appear at $2\theta = 20.19°$ and $21.93°$, respectively, indicating a complete polymorph transformation into cellulose II arrangement. The polymorph for both NCC I and NCC II was maintained after it was being isolated into nanosize fibres using sulphuric acid hydrolisis. As shown in Figure 2, NCC I retains its three peaks at $2\theta = 15.66°$, $16.68°$ and $22.91°$, which confirmed that cellulose I polymorph was maintained. The effect of the mercerisation of MCC II became obvious after it was being isolated into nanosize fibres (NCC II). Even though it maintained the cellulose II pattern, it showed very weak/broad peaks at $2\theta = 20.23°$ and $22.25°$, indicating that the crystallinity of the fibre was greatly affected.
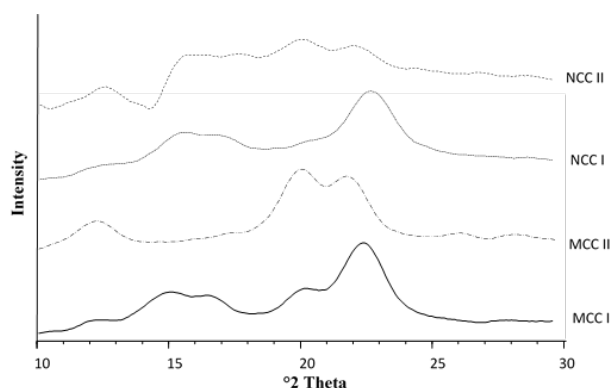
Figure 2. The X-ray diffraction pattern of MCC and NCC with cellulose I and II polymorphs

Table 1 shows the crystallinity index (CI) percentage of both micro and nano fibres. The CI of MCC I was 85.3% and this was decreased after mercerisation into 79.5% in MCC II. The decrement was due to the molecular degradation of cellulose chains as the polymorph rearranged its structure (Borysiak & Garbarczyk, 2003). During mercerisation, alkali penetrates into the fibre bundles and loosens the hydrogen bonding. The fibres then move apart, allowing rearrangement of the structure, and thus, decreasing its crystallinity (El Oudiani et al., 2011, pp. 1221-1229; Gupta et al., 2013, pp. 843-849). The effect of mercerisation seems to be more prominent after being isolated into nanosize. This was shown by a dramatic reduction of CI of NCC II to 55.3% as compared with NCC I (78.0%). As mentioned before, the peak of NCC II seems to be very broad compared to NCC I. The broad peak indicates lower crystallinity (Gupta et al., 2013, pp. 843-849). Many studies have reported that cellulose II is easily hydrolysed than cellulose I (Oh et al., 2005, pp. 417-428; Kuo & Lee, 2009, pp. 41-46; Mittal et al., 2011, p. 41; Song et al., 2015, pp. 164-170). Since the fibril packing of cellulose II has been loosen and contain amorphous region more than cellulose I, it promotes its sensitivity to acid during the hydrolysis.

Table 1

The Crystallinity index (CI) of cellulose I and II of MCC and NCC

Sample	Intensity$_{200}$		Instensity$_{am}$		CI (%)
	2θ	Intensity	2θ	Intensity	
MCC I	22.63	998	18.287	172	85.3
MCC II	21.93	677	18.175	175	79.5
NCC I	22.91	880	18.767	248	78.0
NCC II	22.25	351	18.50	284	55.3

Morphological Analysis (SEM, TEM, FE-SEM)

The morphological analysis of MCC and NCC fibres was taken using various electron microscopes (Figures 3a-h). Both cellulose I and II polymorphs from MCC and NCC were compared at different magnifications. As shown in Figure 3a, the fibres are flat/thin in shape and have a smooth surface. However, after undergoing the the mercerisation treatment, MCC II fibres (Figure 3b) were swollen and the fibre surface became roughened. This swollen phenomenon is known as the effects of mercerisation. As alkali penetrated the microfibril, fibril was swollen and provoked the disruption of fibril packing/assembly. Hence, the gap between the fibrils became obvious and created a rough surface effects. This also has exposed more fibre surface areas and increased the ability of absorption.

The same trend was observed in the TEM images for NCC I and II (Figure 3c – d). As shown in Figure 3c, NCC I fibres isolated from MCC I exhibited a needle/rod-like shape as compared with NCC II which had an irregular rounded-like shape (Figure 3d). Further observations of the FE-SEM images (Figure 3e – h) revealed that NCC II was severely swollen as compared to NCC I. As explained before, MCC II exhibited a rough surface area due to the gap produced by the neighbouring swollen fibrils. Hence, it increased accessibility of acid to

attack the amorphous region during the acid hydrolysis. The amorphous region of MCC II is greater (indicated by its lower CI) than MCC I, and this promoted more hydrolyses, and thus, resulting in NCC II with lower CI. The same trend has also been reported by Sèbe et al. (2012, pp. 570-578) for the NCC fibre produced from different polymorphs of the MCC fibres using Atomic Force Microscope (AFM).
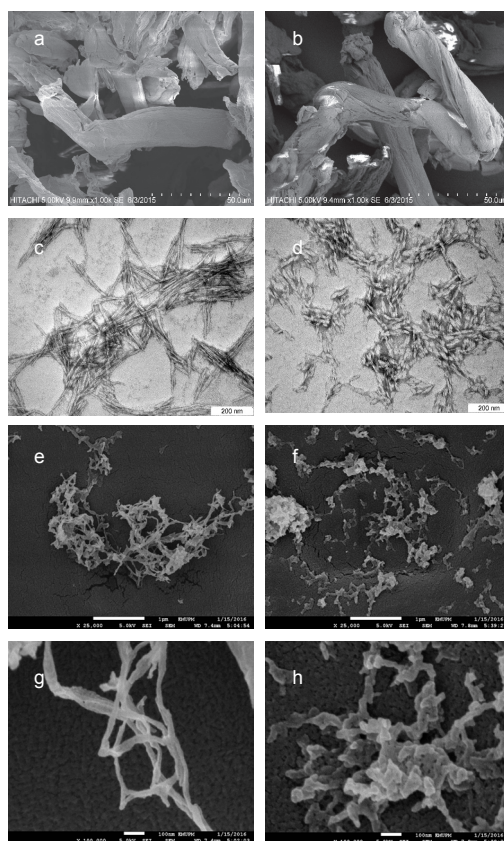
Figure 3. Electron micrographs of micro and nano size cellulose fibres before and after the polymorph conversion (mercerisation) ; SEM images at 1k mag. (a) MCC I (b) MCC II ; TEM images at 100k mag. (c) NCC I and (d) NCC II ; FE-SEM images (e) NCC I at 25k mag., (f) NCC II at 25k mag., (g) NCC I at 100k mag., and (h) NCC II at 100k mag

Dimension, Size Distribution, Zeta Potential and Conductivity Analysis

The purposes of carrying out the dimension analysis were to determine the size of fibres and examine the fibre size distribution. All the MCC and NCC fibres were analysed using two techniques: manual measurement on electron microscope images and also dynamic light scattering (DLS) analysis. Meanwhile, DLS was also used to measure the zeta-potential and conductivity of the NCC fibres.

Fibre Size of MCC and NCC by Manual Measurement

The manual measurement was based on the average reading of 150 measurements of individual fibres. The measurement was to determine the fibre size of MCC before and after the mercerisation and confirm fibre size after the acid hydrolysis (NCC) were in nanosize. The results are presented in Table 2.

Table 2
Dimension of MCC and NCC fibres by manual measurement

Type	Length	Diameter	Length/diameter (l/d) ratio
MCC I	112.3 μm	21.4 μm	5.6
MCC II	78.5 μm	23.4 μm	3.5
NCC I	180.82 nm	11.29 nm	18.18
NCC II	74.04 nm	21.36 nm	3.70

MCC I fibres attained the length of 112.3 μm and diameter of 21.4 μm. However, after the mercerisation (MCC II), and as swollen had taken place, the fibre was shortened by 30% (78.5 μm). However, the diameter was increased by 9% (23.4 μm) as compared to the MCC I fibres. MCC I exhibited a greater l/d ratio (5.6) as compared to MCC II (3.6).

After the hydrolysis, both NCCs were identified as nanofibres (size < 100 nm). However, NCC II was found to be shorten more than half in size (59%) than NCC I. This was due to cellulose II containing more amount of amorphous region. Therefore, it promotes chemical absorption early and allows hydrolysis to occur at a longer period producing shorter fibre (Borysiak & Grząbka-Zasadzińska, 2016). Since the internal surface area of cellulose II was greater than cellulose I, it accelerated chemical penetration during the hydrolysis. On the other hand, NCC II also exhibited a diameter enlargement up to 89% than NCC I which caused an enormous difference in l/d ratio.

Analysis of MCC and NCC fibres by Dynamic Light Scattering (DLS)

As shown in Figure 4a, MCC II generated a bigger diameter fibre distribution than MCC I due to the swelling effect of mercerisation. The mean size for MCC I and MCC II is 47.57 μm and 81.63 μm, respectively. The highest range of the fibre distribution in MCC I was between 34.67 – 45.71 μm, which represents 6.53% of the total distribution. Meanwhile, MCC II had the highest range comprised fibre from 69.18 – 91.20 μm, which represents 7.02% of the total measurement. In term of homogeneity, MCC II was found to produce more homogenous fibre size as compared with MCC I, as indicated by the distribution curve shown in Figure 4a.

The same trend was also observed for the NCC fibre shown in Figure 4b. NCC I hasa smaller mean diameter size of 197 nm compared to NCC II that produced a larger mean diameter size of 216.4 nm. Both NCCs also have low zeta potential, which is -8.66 mV for NCC I and -7.99 mV for NCC II. The conductivity was also recorded to be very low for both NCC I and NCC II, with the conductivity value of 0.0629 mS/cm and 0.0744 mS/cm, respectively.
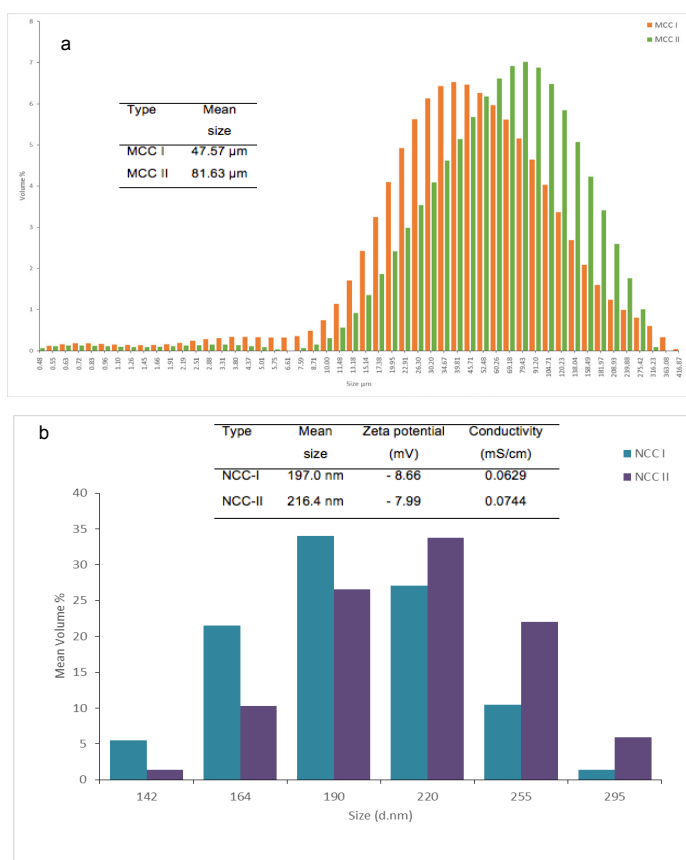
Figure 4. The Dynamic Light Scattering (DLS) analysis of (a) MCC and (b) NCC fibres

Figure 5 shows the thermo-gravimetric (TG) and derivative thermo-gravimetric (DTG) curves of MCC and NCC. Only a single pyrolysis process was involved for MCC, whereas NCC has two distinctive pyrolysis steps. The first-step pyrolysis for NCC occurred in between 150 to 250°C, which corresponded to moisture evaporation (George et al., 2005, pp. 189-194; Yue et al., 2012, pp. 1173-1187) and sulphate groups on the crystal surface (Wang et al., 2007, pp. 3486-3493; Yue et al., 2012, pp. 1173-1187). Since NCC possessed a larger surface area, it increased the absorption properties and contained more moisture than MCC. The degradation of cellulose occurred between 250 to 500°C.
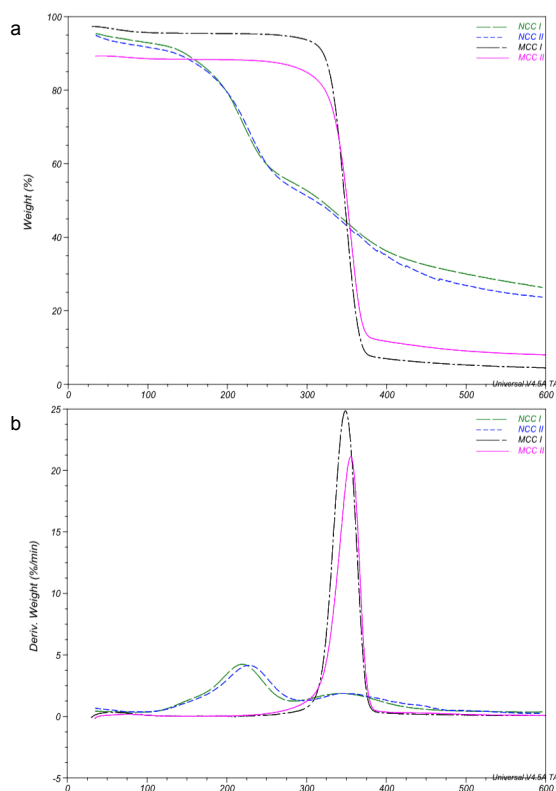
Figure 5. The thermal stability of MCC and NCC fibres (a) TG and (b) DTG curves

The thermal properties values of MCC and NCC are shown in Table 3. Both cellulose II polymorph fibres (MCC II and NCC II) showed higher decomposition temperatures than cellulose I polymorph fibres (MCC I and NCC I). The decomposition temperature of MCC I was 329.28°C, and this was increased to 332.53°C for MCC II. Meanwhile, the same trend was also observed for NCC I which had 315.52°C as its decomposition temperature and this increased to 325.40°C in NCC II. The thermal stability of cellulose II is better than cellulose I; this was attributed to the strong inter and intra bonding of –OH groups in cellulose II, which accounted to a greater amount of energy required to start thermal degradation process (Yue et al., 2012, pp. 1173-1187).

In term of weight loss and residue, MCC II exhibited less weight loss (76.46%) but with higher residue (8.02%) compared with MCC I with 89.03% weight loss and 4.48% residue. The residue had shown the level of β-glycosidic linkages. Stable structure such as cellulose II exhibited more residue formation (Abbott & Bismarck, 2010, pp. 779-791).

In contrast, NCC II fibre obtained greater weight loss in both the two-step pyrolysis (40.03% and 24.42%) with less residue (23.71%) compared with NCC I fibre; 38.70% and 23.21% for weight loss and 26.36% residue. As mentioned before, NCC II was more moisture-sensitive and contained a great amount of moisture. This was shown by a large weight loss in the first step of pyrolysis, which corresponded to the moisture evaporation. NCC II contained excessive amount of amorphous chains; therefore, it accelerated cellulose molecule decomposition (indicated by its higher weight loss in the second pyrolysis) and reduced the residue amount.

Table 3
The thermal properties of MCC and NCC fibres

Fibre Type	Tdec (°C)		Weight Loss (%)		Residue (%)
MCC I	329.38		89.03		4.48
MCC II	332.53		76.46		8.02
NCC I	176.25	315.52	38.70	23.21	26.36
NCC II	181.72	325.40	40.03	24.42	23.71

CONCLUSION

From the study, it can be concluded that the mercerisation treatment conducted on native MCC using 20% of NaOH concentration had completely transformed cellulose I into cellulose II polymorph. However, mercerisation was also found to decrease the CI of MCC II. The effect of mercerisation found to be more excessive after acid hydrolysis. The CI of NCC II was tremendously affected as the mercerisation treatment apparently had promoted disruption of crystalline region during the hydrolysis. Electron micrographs revealed that both cellulose II polymorph fibres (MCC II and NCC II) were morphologically affected. MCC II showed a swollen and rough fibre surface, while NCC II exhibited an irregular rounded-like shape fibre compared with NCC I which appeared as needle/rod-like shape fibres. The analysis of size distribution and dimension measurement confirmed that the mercerisation treatment caused increment in the fibre's diameter but at the same time, shortened the length which is responsible for the significant difference in l/d ratio. The thermal analysis showed that both cellulose II polymorph fibres (MCC II and NCC II) exhibited better thermal stability compared to cellulose I polymorph fibres.

REFERENCES

Abbott, A., & Bismarck, A. (2010). Self-reinforced cellulose nanocomposites. *Cellulose, 17*(4), 779-791.

Bondeson, D., Mathew, A., & Oksman, K. (2006). Optimization of the isolation of nanocrystals from microcrystalline cellulose by acid hydrolysis. *Cellulose, 13*(2), 171-180.

Borysiak, S., & Doczekalska, B. (2008). Research into the mercerization process of beech wood using the WAXS method. *Fibres and Textiles in Eastern Europe, 6*(71), 101-103.

Borysiak, S., & Garbarczyk, J. (2003). Applying the WAXS method to estimate the supermolecular structure of cellulose fibers after mercerization. *Fibres and Textiles in Eastern Europe, 11*(5), 104-106.

Borysiak, S., & GrzabkaZasadzińska, A. (2016). Influence of the polymorphism of cellulose on the formation of nanocrystals and their application in chitosan/nanocellulose composites. *Journal of Applied Polymer Science, 133*(3), 1-9.

Dinand, E., Vignon, M., Chanzy, H., & Heux, L. (2002). Mercerization of primary wall cellulose and its implication for the conversion of cellulose I→ cellulose II. *Cellulose, 9*(1), 7-18.

El Oudiani, A., Chaabouni, Y., Msahli, S., & Sakli, F. (2011). Crystal transition from cellulose I to cellulose II in NaOH treated Agave americana L. fibre. *Carbohydrate Polymers, 86*(3), 1221-1229.

Gatenholm, P., & Klemm, D. (2010). Bacterial nanocellulose as a renewable material for biomedical applications. *MRS Bulletin, 35*(03), 208-213.

George, J., Ramana, K. V., Sabapathy, S. N., Jagannath, J. H., & Bawa, A. S. (2005). Characterization of chemically treated bacterial (Acetobacter xylinum) biopolymer: Some thermo-mechanical properties. *International Journal of Biological Macromolecules, 37*(4), 189-194.

Gupta, P. K., Uniyal, V., & Naithani, S. (2013). Polymorphic transformation of cellulose I to cellulose II by alkali pretreatment and urea as an additive. Carbohydrate Polymers, 94(2), 843-849.

Habibi, Y., Lucia, L. A., & Rojas, O. J. (2010). Cellulose nanocrystals: chemistry, self-assembly, and applications. *Chemical Reviews, 110*(6), 3479.

Jin, E., Guo, J., Yang, F., Zhu, Y., Song, J., Jin, Y., & Rojas, O. J. (2016). On the polymorphic and morphological changes of cellulose nanocrystals (CNC-I) upon mercerization and conversion to CNC-II. *Carbohydrate Polymers, 143*, 327-335.

Jonoobi, M., Oladi, R., Davoudpour, Y., Oksman, K., Dufresne, A., Hamzeh, Y., & Davoodi, R. (2015). Different preparation methods and properties of nanostructured cellulose from various natural resources and residues: a review. *Cellulose, 22*(2), 935-969.

Kenji, K. (2005). *Cellulose and cellulose derivatives: molecular characterisation and its applications*. Amsterdam: Elsevier Science.

Kuga, S., Takagi, S., & Brown, R. M. (1993). Native folded-chain cellulose II. *Polymer, 34*(15), 3293-3297.

Kumar, V., de la Luz Reus-Medina, M., & Yang, D. (2002). Preparation, characterization, and tableting properties of a new cellulose-based pharmaceutical aid. *International Journal of Pharmaceutics, 235*(1), 129-140.

Kuo, C. H., & Lee, C. K. (2009). Enhancement of enzymatic saccharification of cellulose by cellulose dissolution pretreatments. *Carbohydrate Polymers, 77*(1), 41-46.

Langan, P., Nishiyama, Y., & Chanzy, H. (1999). A revised structure and hydrogen-bonding system in cellulose II from a neutron fibre diffraction analysis. *Journal of the American Chemical Society, 121*(43), 9940-9946.

Liu, D., Song, J., Anderson, D. P., Chang, P. R., & Hua, Y. (2012). Bamboo fibre and its reinforced composites: structure and properties. *Cellulose, 19*(5), 1449-1480.

Liu, Y., & Hu, H. (2008). X-ray diffraction study of bamboo fibres treated with NaOH. *Fibres and Polymers, 9*(6), 735-739.

Lu, P., & Hsieh, Y. L. (2010). Preparation and properties of cellulose nanocrystals: rods, spheres, and network. *Carbohydrate Polymers, 82*(2), 329-336.

Ma, H., Zhou, B., Li, H. S., Li, Y. Q., & Ou, S. Y. (2011). Green composite films composed of nanocrystalline cellulose and a cellulose matrix regenerated from functionalized ionic liquid solution. *Carbohydrate Polymers, 84*(1), 383-389.

Mansikkamäki, P., Lahtinen, M., & Rissanen, K. (2005). Structural changes of cellulose crystallites induced by mercerisation in different solvent systems; determined by powder X-ray diffraction method. *Cellulose, 12*(3), 233-242.

Mittal, A., Katahira, R., Himmel, M. E., & Johnson, D. K. (2011). Effects of alkaline or liquid-ammonia treatment on crystalline cellulose: changes in crystalline structure and effects on enzymatic digestibility. *Biotechnology for Biofuels, 4*(1), 41-56.

Oh, S. Y., Yoo, D. I., Shin, Y., & Seo, G. (2005). FTIR analysis of cellulose treated with sodium hydroxide and carbon dioxide. *Carbohydrate Research, 340*(3), 417-428.

Prasanth, R., Nageswaran, S., Thakur, V. K., & Ahn, J. H. (2015). Electrospinning of Cellulose: Process and Applications. In V. K. Thakur (Ed.), *Nanocellulose Polymer Nanocomposites: Fundamentals and Applications* (pp. 311-340). USA: John Wiley & Sons, Inc.

Puglia, D., Fortunati, E., Santulli, C., & Kenny, J. M. (2014). Multifunctional Ternary Polymeric Nanocomposites Based on Cellulosic Nanoreinforcements. In V. K. Thakur (Ed.), *Nanocellulose Polymer Nanocomposites: Fundamentals and Applications* (pp. 163-198). USA: John Wiley & Sons, Inc.

Revol, J. F., Dietrich, A., & Goring, D. A. I. (1987). Effect of mercerization on the crystallite size and crystallinity index in cellulose from different sources. *Canadian Journal of Chemistry, 65*(8), 1724-1725.

Sèbe, G., Ham-Pichavant, F., Ibarboure, E., Koffi, A. L. C., & Tingaut, P. (2012). Supramolecular structure characterization of cellulose II nanowhiskers produced by acid hydrolysis of cellulose I substrates. *Biomacromolecules, 13*(2), 570-578.

Segal, L. G. J. M. A., Creely, J. J., Martin Jr, A. E., & Conrad, C. M. (1959). An empirical method for estimating the degree of crystallinity of native cellulose using the X-ray diffractometer. *Textile Research Journal, 29*(10), 786-794.

Silva, T. C. F., Silva, D., & Lucia, L. A. (2015). The Multifunctional Chemical Tunability of Wood-Based Polymers for Advanced Biomaterials Applications. In V. K. Thakur & M. R. Kessler (Eds.), G*reen Biorenewable Biocomposites: From Knowledge to Industrial Applications* (pp. 427-459). Canada: Apple Academic Press.

Široký, J., Blackburn, R. S., Bechtold, T., Taylor, J., & White, P. (2010). Attenuated total reflectance Fourier-transform Infrared spectroscopy analysis of crystallinity changes in lyocell following continuous treatment with sodium hydroxide. *Cellulose, 17*(1), 103-115.

Song, Y., Zhang, J., Zhang, X., & Tan, T. (2015). The correlation between cellulose allomorphs (I and II) and conversion after removal of hemicellulose and lignin of lignocellulose. *Bioresource Technology, 193*, 164-170.

Wang, H., Li, D., Yano, H., & Abe, K. (2014). Preparation of tough cellulose II nanofibers with high thermal stability from wood. *Cellulose, 21*(3), 1505-1515.

Wang, N., Ding, E., & Cheng, R. (2007). Thermal degradation behaviour of spherical cellulose nanocrystals with sulfate groups. *Polymer, 48*(12), 3486-3493.

Wertz, J. L., Mercier, J. P., & Bédué, O. (2010). *Cellulose science and technology*. USA: CRC Press.

Yue, Y. (2011). *A comparative study of cellulose I and II fibres and nanocrystals*. (Doctoral dissertation). Louisiana State University.

Yue, Y., Han, J., Han, G., Zhang, Q., French, A. D., & Wu, Q. (2015). Characterization of cellulose I/ II hybrid fibers isolated from energycane bagasse during the delignification process: morphology, crystallinity and percentage estimation. *Carbohydrate Polymers, 133*, 438-447.

Yue, Y., Zhou, C., French, A. D., Xia, G., Han, G., Wang, Q., & Wu, Q. (2012). Comparative properties of cellulose nano-crystals from native and mercerized cotton fibers. *Cellulose, 19*(4), 1173-1187.